Permafrost Degradation Pathways during the 21 st Century of High-elevated Rock Ridge in the Mont Blanc Massif

Florence Magnin, Benjamin Pohl, Jean-Yves Josnin, Julien Pergaud, Philip Deline, Ludovic Ravanel

Permafrost Degradation Pathways during the 21st Century of High-elevated Rock Ridge in the Mont Blanc Massif

Florence Magnin[1], Benjamin Pohl[2], Jean-Yves Josnin[1], Julien Pergaud[2], Philip Deline[1], Ludovic Ravanel[1]

[1] Laboratoire EDYTEM, UMR5204, CNRS, Université Savoie Mont Blanc, Le Bourget du Lac, France

[2] Biogéosciences, UMR6282, CNRS, Université Bourgogne Franche-Comté, Dijon, France

Abstract

Rockwall permafrost is increasingly investigated because of its possible role in bedrock failure, related hazards and geotechnical practices. In this study, we simulate the possible permafrost pathways during the 21st century of one of the coldest rock ridge in the European Alps: the Grand Pilier d'Angle (4305 m a.s.l). Rockwalls permafrost evolution is primarily driven by air temperature and we thus run simulations with 13 climate models declined with the most contrasted greenhouse gas emissions scenarios (RCP2.6 and 8.5) until 2100 to account for climate models uncertainty. Results show that by 2050 permafrost would have warmed by about 1°C down to 35 m depth compared to 2020, and that about 50, and 30 % of this perturbation will reach depths of 80 and 130 m respectively. But uncertainty remains rather high before mid-century and possible permafrost pathways are more reliable after 2050. By the end of the century, a "business as usual" scenario would result in a surge in permafrost degradation with +3 ±1.3 and +1.4 ±0.6 °C at 35 m and 130 m depth respectively. In narrow topographies where heat fluxes from opposite faces merge such as the top of our study site, the temperature increase would be enhanced, reaching +4°C ±1.9°C. In this scenario, permafrost would thaw in most alpine rockwalls except shaded rock faces > 4000 m a.s.l. that are several tens to hundreds of meters apart from sun-exposed faces such as the north face of our study site. Conversely, drastic reduction in greenhouse gas emissions would result in a stabilization in permafrost degradation, restricting bedrock thawing to sun-exposed and shaded faces below 4000 and 3000 m a.s.l. respectively, where warm permafrost is currently present.

Introduction

Permafrost (*i.e.* ground that remains at or below 0°C for at least two consecutive years[1]) is commonly regarded as a geological manifestation of climate. In this respect, the evolution of its temperature is recognized as an Essential Climate Variable by the Global Climate Observation System (GCOS) and is thus monitored throughout the world by the Global Terrestrial Network for Permafrost (GTN-P). In the frame of this monitoring, temperature collected into boreholes within the last decade has shown a general warming of about +0.19 ± 0.05°C to +0.39 ± 0.15°C, depending on regions[2]. Locally, permafrost evolution does not only depend on regional climate but also on ground type and permafrost temperature (i.e. more or less close to 0°C). The closer to 0°C and the greater the ice content, the more delayed its response to warming signal due to latent heat consumption[3]. For this reason, bedrock permafrost is particularly sensitive to air temperature because of its relatively low ice content, which is restrained to pore space and fractures. In alpine environment, the sensitivity of rockwall permafrost to air temperature is furthermore exacerbated by the topographical settings, as steepness favors a direct coupling with the atmosphere, due to limited accumulation of snow or debris, and because of the multi-sided heat propagation in peaks, ridges and spurs[4].

Permafrost ice is also a key component for ground mechanical properties and rheology[5,6], and is thus of concern for geotechnical engineering practices[7,8]. Since the remarkably high number of rockfalls observed during the heat wave that struck the European Alps in summer 2003[9], systematic observations have shown that low magnitude rockfalls (a few tens to a few hundreds of cubic meters) mostly occur during hot summers[10,11]. The role of permafrost is also suggested by frequent observations of ice in rockfall scars, hinting at laboratory studies that showed the physical and mechanical alteration of ice-filled fractures cementing bedrock compartments when warming towards 0°C[6,12,13]. The recent increase in periglacial rock slope failures is consequently attributed to permafrost degradation[10,14] and rises concerns for alpine communities as it jeopardizes mountain practices, professions and infrastructure[15–17]. In a further extent, rockfalls detached from high-elevation rockwalls may threaten people and infrastructure down to the valley floor by provoking high magnitude hazard cascades[18–21]. Indeed, in high mountain environments, rockfalls may impact sediment storages, lakes or glaciers and trigger the sudden displacement of high volumes of non-consolidated materials. Such catastrophic chains of processes constitute a new threat in deglaciating lansdcapes[22]. In this context, estimating the evolution of rockwall permafrost throughout the 21st century is crucial to anticipate hazardous areas and bears strong implications for land planning, risk mitigations and practice adaptations.

Due to its enhanced sensitivity to climate signal, rockwall permafrost evolution is primarily driven by air temperature and local topographical settings. Thus, the realism of permafrost projections strongly relies on the skill of climate models. Within the 5th Coupled Model Intercomparison Project (CMIP5[23]) of the IPCC 5th Assessment Report (AR5[24]), fully coupled climate models were forced by idealized

radiative forcing approximating anthropogenic greenhouse gas emissions. These scenarios, named Representation Concentration Pathways (RCPs), correspond to additional radiative forcing of +2.6 to +8.5 $W.m^{-2}$ by 2100 compared to the pre-industrial era. Considering an ensemble of climate models is necessary to quantify the model dependency of the results, and thus, the uncertainties associated with the climate change projections. However, these models have rather coarse spatial resolutions (typically, a few tens of kilometers) that make their use for impact studies rather difficult, especially in complex environments like mountain massifs. Thus, efforts are conducted to provide downscaled climate projections at high spatial resolution in realistic topographical settings for the coming decades. Recently, Joly et al.[25] have downscaled 13 models taken from the CMIP5 modeling exercise under the most contrasted scenarios (namely, RCP2.6 and 8.5) in the Mont Blanc massif (Northwestern European Alps; MBM hereafter) at a spatial resolution of 200 × 200 m. Their results show major decrease in frost frequency over and around the Mont Blanc summit[26]. These results provide a unique opportunity to assess how climate pathways could affect rockwall permafrost within the 21st century.

In this study, we run simulations of permafrost evolution at the Grand Pilier d'Angle site (4305 m a.s.l.) in the MBM (Fig. 1) by combining mean annual rock surface temperature distribution (MARST) statistically determined from air temperature and potential incoming solar radiation[27] (Fig. 1e) with the physic-based Feflow® (DHI-WASY) modeling tools, to simulate heat conduction and latent heat processes[28]. These simulations are forced by the aforementioned downscaled CMIP5 projections under RCP2.6 and 8.5.

The Grand Pilier d'Angle is the outermost part of the ridge extending eastwards of the Mont Blanc summit (4809 m a.s.l.). Its north and east faces respectively stand 700 and 1000 m above the Brenva glacier, while its south face dominates the summital cirque of the Frêney glacier by about 200 m height. A part of its north face is covered by a hanging glacier witnessing of cold permafrost (< -2°C) occurrence, which is also suggested by the permafrost map produced by Magnin et al. [27] (Fig. 1e and 2a). Its east face has been affected by several rock avalanches within the 2Oth century, with a succession of five events in November 1920 with a total rock volume around 3×10^6 m^3, and a similar magnitude event in January 1997 [29, 30]. Despite the historical recurrence of such hazards, the Grand Pilier d'Angle is famous for his highly challenging climbing routes.

This site was chosen as a theoretical study-case because (i) its high elevation guarantees that permafrost will persist by the end of the 21st century[28], (ii) its > 300 m wide basis helps in disentangling the respective effects of the climate signal and topographical perturbation in the temperature evolution, and (iii) its narrow summit is representative of high alpine rockwalls, where temperature reflects the enhanced and mixed lateral heat fluxes coming from the opposite rock faces[4]. Such topographical characteristics allow us to assess the broad significance of the results for high-alpine permafrost evolution pathways.

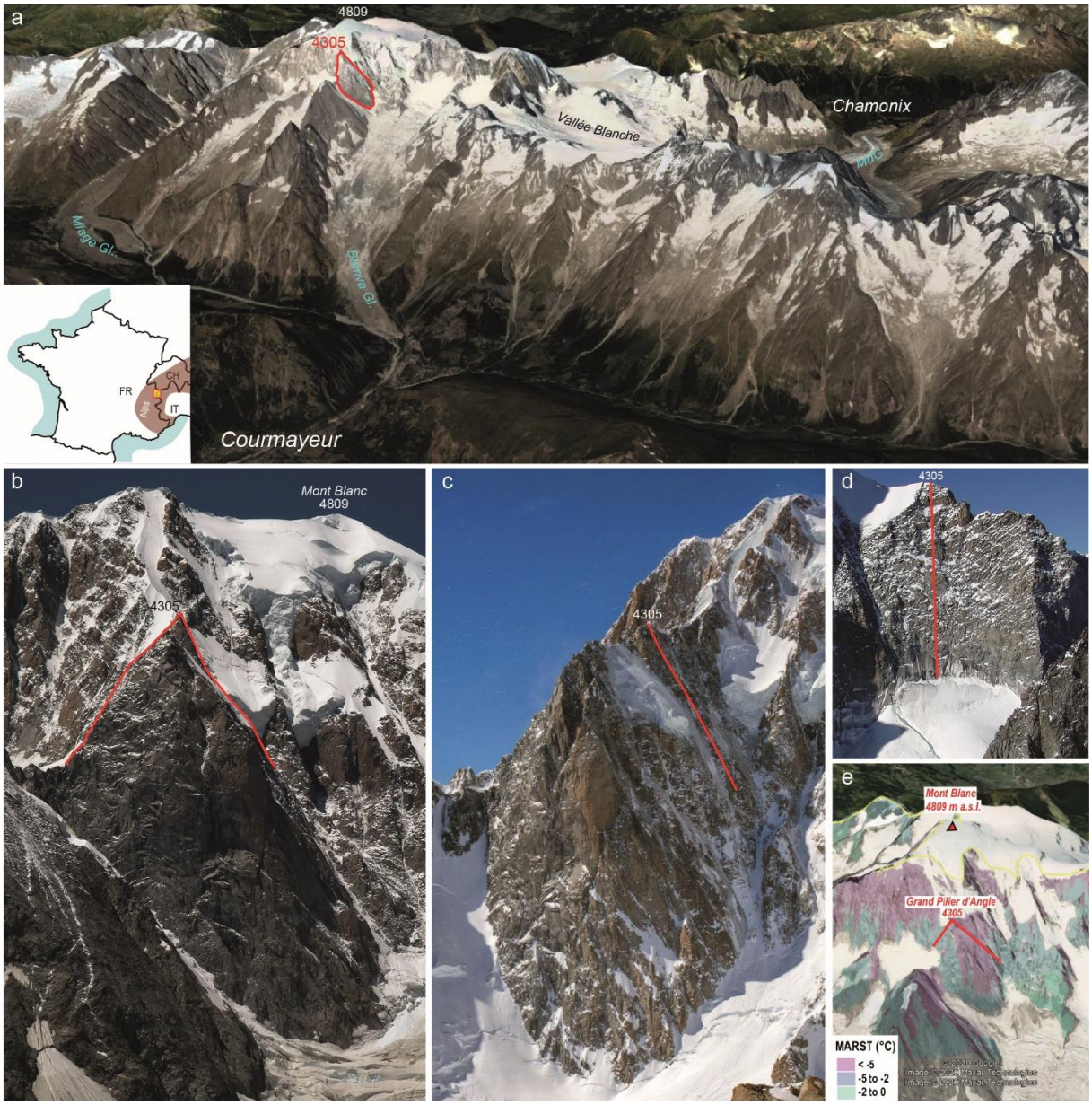

Figure 1. a. Location of the Grand Pilier d'Angle (red polygon) in the Mont Blanc massif (Google Earth image). **b.** Profile on South face (on left) and North face (on right) of the GPA. **c.** North face of the GPA. **d.** South face of the GPA. **e**. Mean Annual Rock Surface Temperatures (MARST) at the GPA mapped by Magnin et al.[27]. Elevations in m a.s.l.

Modeling the rockwall temperature evolution

Rockwall temperature modeling is a common tool to investigate permafrost dynamics and predict evolutions at mountain sites[4,28,31–34]. In a first step, rock surface temperature time series are obtained by mean of energy balance modeling, measurements, or statistical relationship between rock surface temperature, air temperature, incoming solar radiation and snow depth. These time series are then used to calculate heat transfers from surface to depth, by generally considering heat conduction and latent

heat processes into a homogeneous, isotropic and saturated rock media with a higher porosity value than in natural rock to indirectly account for ice or water content in fractures. Complex convective heat transfer processes possibly induced by water percolation or air ventilation into bedrock fractures[35,36] are assumed to play a secondary role in pluri-decadal permafrost evolution and are thus overlooked in such approaches.

In the MBM, Magnin et al.[27] have mapped the (MARST (Fig. 1e) by mean of average potential incoming solar radiation at the rock surface and air temperature of the period 1961-1990. By using measured and reconstructed air temperature time series, Magnin et al.[28] have later simulated the past evolution of rockwall permafrost between the end of the Little Ice Age (1850) and the present time for N-S profiles of three sites distributed along an altitudinal profile in the MBM, including the Grand Pilier d'Angle. This study has shown that modeled temperature match measured temperature in 10 m deep boreholes for depths > 8 m. Authors also proposed a preliminary projection for permafrost evolution by the end of the 21st century, showing that, under RCP8.5, permafrost will likely subsist only at the Grand Pilier d'Angle, the highest-elevated study site. These projections were based on the IPSL-CM5A-MR model run at a spatial resolution of 1.25 × 2.5° (that is roughly 140 × 200 km at this latitude, one of the highest spatial resolutions available among the CMIP5 ensemble). Orographic effects on the local climate were still largely insufficient to produce realistic climate boundary conditions to force rockwall permafrost simulations. Here, we apply the same modelling approach (details in Supplementary materials S1) to the Grand Pilier d'Angle site (Fig. 1) with the downscaled CMIP5 ensemble.

To ensure model comparability throughout the 21st century and account for uncertainty in our conclusions, climate models are run from 2006 only (Fig. 2a), while the air temperature history – required to initialize permafrost conditions prior to 2006 – is identical for all models and based on assumptions (-1°C in 1850 compared to 1961) and local temperature observations (from 1961 to 2006) similarly to Magnin et al.[28].

Permafrost evolution is then analyzed by mean of respectively 9 and 20 observation points spread along two crosscutting profiles (Fig. 2a). Shallowest points are located at 10 m depth below the SE and NW faces as bedrock temperature near the surface is influenced by a variety of processes not accounted for in our modelling approach. We register simulated bedrock temperature at each time step for each of these observation points and use the simulated time series to analyze permafrost evolution in details while 2D images are extracted the 1st March and 1st September of the years 2015, 2035, 2050, 2075 and 2100.

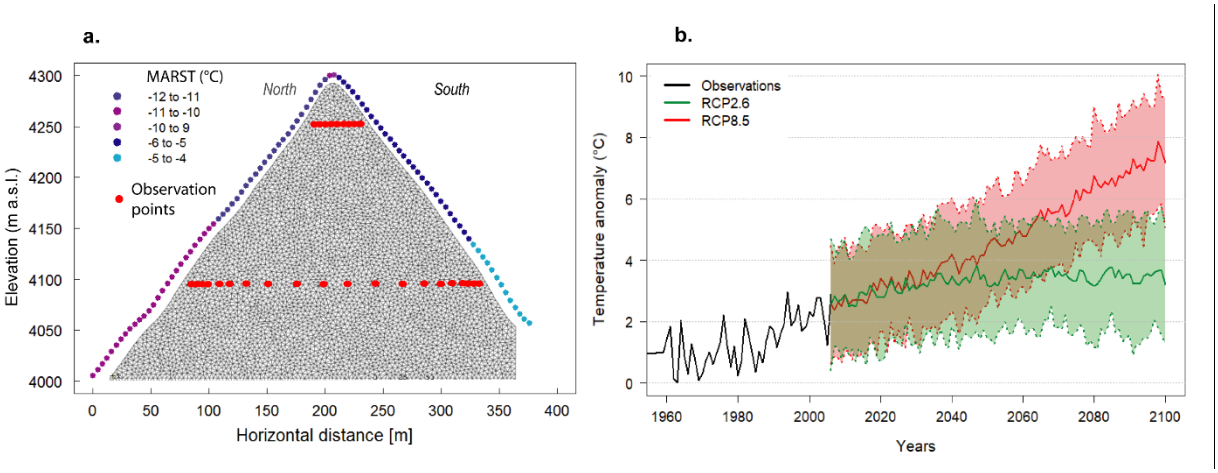

Figure 2. a. Model geometry of the Grand Pilier d'Angle (a 5 km box is drawn below and crossed by the geothermal heat flux, not shown here; see S1 in the Supplements) with initial MARST and observation points recording simulated temperature at each time step. **b.** Local air temperature anomaly pathways (compared to 1961-1990 as calculated by Magnin et al.[27]) under RCP8.5 and 2.6 applied to the initial MARST. The thick lines show the means of the 13 models while the filled areas set the ± 1 standard deviation around the mean to account for models uncertainty.

No distinctive pathways in rockwall permafrost evolution prior to 2050

Air temperature trends are very similar between RCP2.6 and RCP8.5 until 2035 (Fig. 2a) and distinctive pathways only appear between 2035 and 2050. RCP8.5 increasingly differentiates from RCP2.6 during the second half of the century, when the radiative forcings themselves strongly differ. The strong decrease in anthropogenic greenhouse gas emissions in RCP2.6 leads to a rapid stabilization of air temperature, while the latter continuously increases under RCP8.5, in line with rather similar trajectories in corresponding greenhouse gas concentrations.

The consequence of these uniform air temperature trends is that permafrost evolution is similar whatever the considered scenario until 2050 (Fig. 3a-d). In 2020, the first 15 years of climate projections have impacted the bedrock temperature down to about 80 m depth (Fig. 3b). Close to the top, where the ridge is narrow, the bedrock temperature is thus entirely controlled by the different climate models and scenarios which respective propagation from the SE and NW faces add up at the core (Fig. 3a). Transient effects of the historical data have a marginal influence for narrow (< 80 m wide) ridges or peaks and bedrock temperature is thus in a certain equilibrium with recent climate evolution. This is notably revealed by the steady temperature gradient between N and S faces, depicting near vertical isotherms such as shown in idealized steady state cases[4]. The slightly higher temperature for RCP2.6 than the one of RCP8.5 is

consequently reflecting the past 15 years of climate projections and the little influence of radiative forcing at this time. Conversely, the core of the bottom profile remains isolated from the thermal disturbance induced from 2006 until 2050 (Fig. 3b, d) in reason of its remoteness from the surface (> 140 m below the NW and SE surfaces) and the slow heat propagation throughout the bedrock medium.

When comparing the averaged trends of 2020 and 2050, bedrock temperature has increased by 1 ±1 °C at 35 m depth, 0.5 ±0.5 and 0.3 ±0.3 °C at 80 and 130 m depth respectively for RCP8.5. The top profile is marked by a 1.1 ± 1.4°C increase in average (Fig. 3g-h) and uncertainty remains fairly high within this horizon. It however appears very unlikely that the highest part of the ridge will start to thaw before mid-century, with respectively 1 model out of 13 showing positive temperature at 10 m depth in the SE face under RCP2.6, and none under RCP8.5 (Fig. 4). Thawing may possibly occur at the foot of the SE face according to the three warmest predictions of each RCP. It may reach a maximum of 15-20 m depth by 2050, according to the warmest predictions, but > 75 % of the models predict the absence of thawing. Major changes will rather occur within the second half of the 21st century.

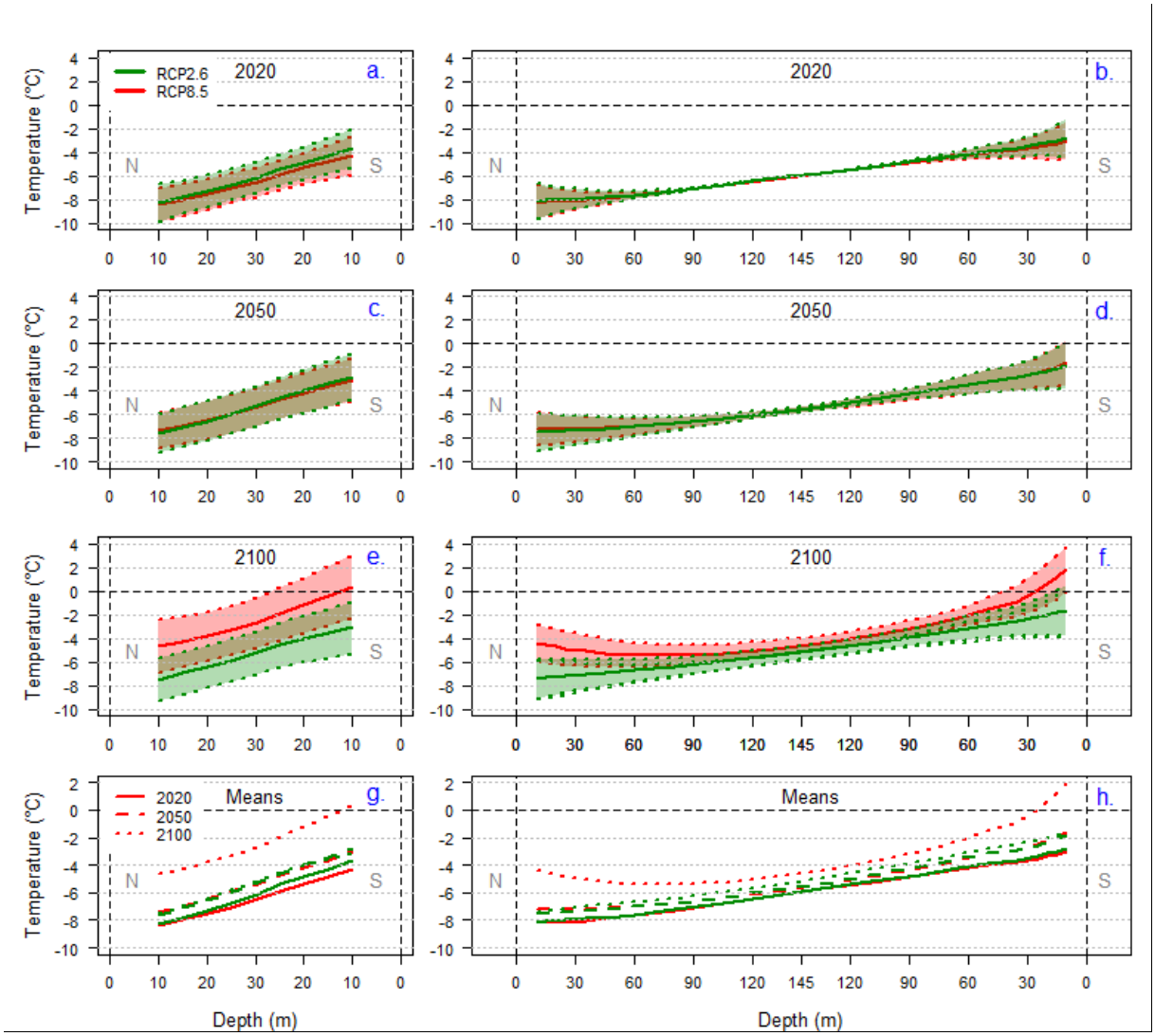

Figure 3. Permafrost temperature pathways from 10 m depth to the core of the rock mass in the top profile (left) and the bottom profile (right). Profile locations are shown on Figure 1.Thick lines are the means of the 13 models while the dashed lines represent the 68 % confidence interval.

Pathways stabilizing versus surging by 2050

By 2050, the effect of the different RCPs becomes clearly predominant upon internal climate variability, and has a strong impact on permafrost degradation pathways. Under RCP2.6, the permafrost evolution almost reaches an equilibrium by 2050, as revealed by identical averaged temperature trend in the top profile between 2050 and 2100 (Fig. 3g), steady temperature gradient from the N to the S face (Fig. 3h), and the near vertical isotherms close to the top (Fig. 5b)[4]. Because of this temperature balancing, the average temperature slightly increases between 2050 and 2100 in the core of the bottom profile, as a result of transient effects of the first half of the 21st century.

Conversely to RCP2.6, RCP8.5 results in major temperature changes within the second half of the 21st century. It will reach +4 ± 1.9 °C compared to 2020 in the top profile in 2100 compared to 2020, +3 ±1.3, +1.8 ± 0.8 and +1.4 ±0.6 °C at 35 m, 80 and 130 m depth respectively in the bottom profile. When considering the 68 % confidence interval, the average warming is well higher than the 68% confidence interval (Fig. 3 c-h). When considering a higher confidence interval, one of the colder RCP8.5 models (95 % confidence interval) displays significant permafrost thawing on the S face, while this only occurs with the warmer RCP2.6 model. (Fig. 5b, d). The warmer climate models (95 % confidence interval) result in similar temperature field patterns on the S face for both scenarios but a significant curling up of the -4°C isotherm below the N face under RCP8.5 (Fig. 5c, f).

Permafrost thawing still remains very unlikely under RCP2.6, even though it slightly progresses down to 25 m depth in the top profile for the warmest prediction as a delayed response to thermal perturbation from the previous decades (Fig. 3e, 4). However, permafrost thawing becomes very likely under RCP8.5 as 50 % of the models predict positive temperature down to 25 m depth by 2100 in the S side of the bottom profile (Fig. 4). Closer to the surface, permafrost thawing is predicted by > 90 % of the RCP8.5 models. The warmest RCP8.5 model even predicts permafrost thawing at a depth of 45 m for the bottom profile and down to the core of the top profile in the SE side by the end of the 21st century. By contrast, the N face will remain frozen in any case due to its very cold state at present time.

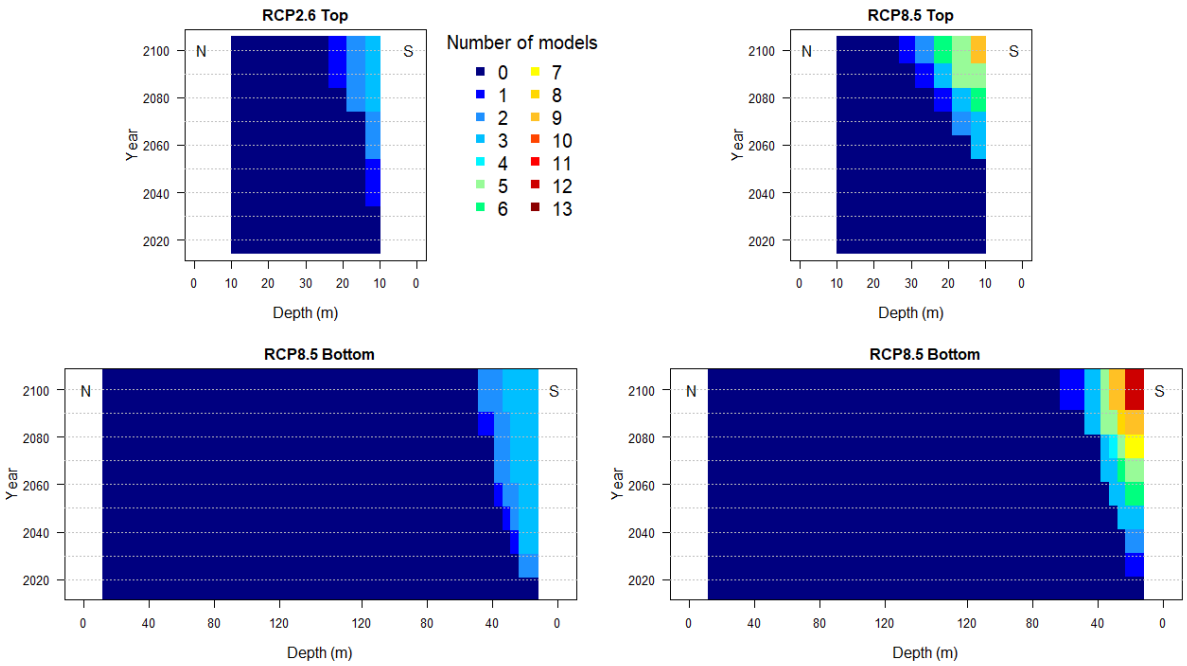

222

223 **Figure 4.** Number of models predicting permafrost thawing (i.e. mean annual temperature
224 becomes positive) for both profiles and both RCPs according to depth, time and aspect.

225

226 Figure 5 further shows that the average and colder models (within the 95 % confidence interval)
227 have significantly different temperature fields according to RCP. The colder RCP8.5 will result
228 in a substantial permafrost thawing and warm permafrost progression below the entire S face
229 (Fig. 5d) which will remain in cold permafrost conditions for the same colder model forced
230 with RCP2.6 (Fig. 5a). Similarly, the average model shows a certain thermal equilibrium and
231 warm permafrost only at the foot of the S face under RCP2.6 (Fig. 5b), but a substantial
232 shrinking of the cold permafrost body (-5°C isotherm) and a significant deepening of permafrost
233 thawing and warm permafrost when forced with RCP8.5 (Fig. 5e). These latter patterns
234 (significant permafrost thawing and warm permafrost progression) are actually similar for the
235 three RCP8.5 models, witnessing of their reliability under a scenario of enhanced anthropogenic
236 greenhouse gas emissions. However, affected depths are about twice greater with the warmer
237 model compared to the colder, and this result in permafrost disappearance at the top of the
238 Grand Pilier d'Angle with the former, due to the predominance of lateral heat fluxes from the
239 S face[4] – a pattern which is also found for the same model under RCP2.6 (Fig. 5, c, f).

240

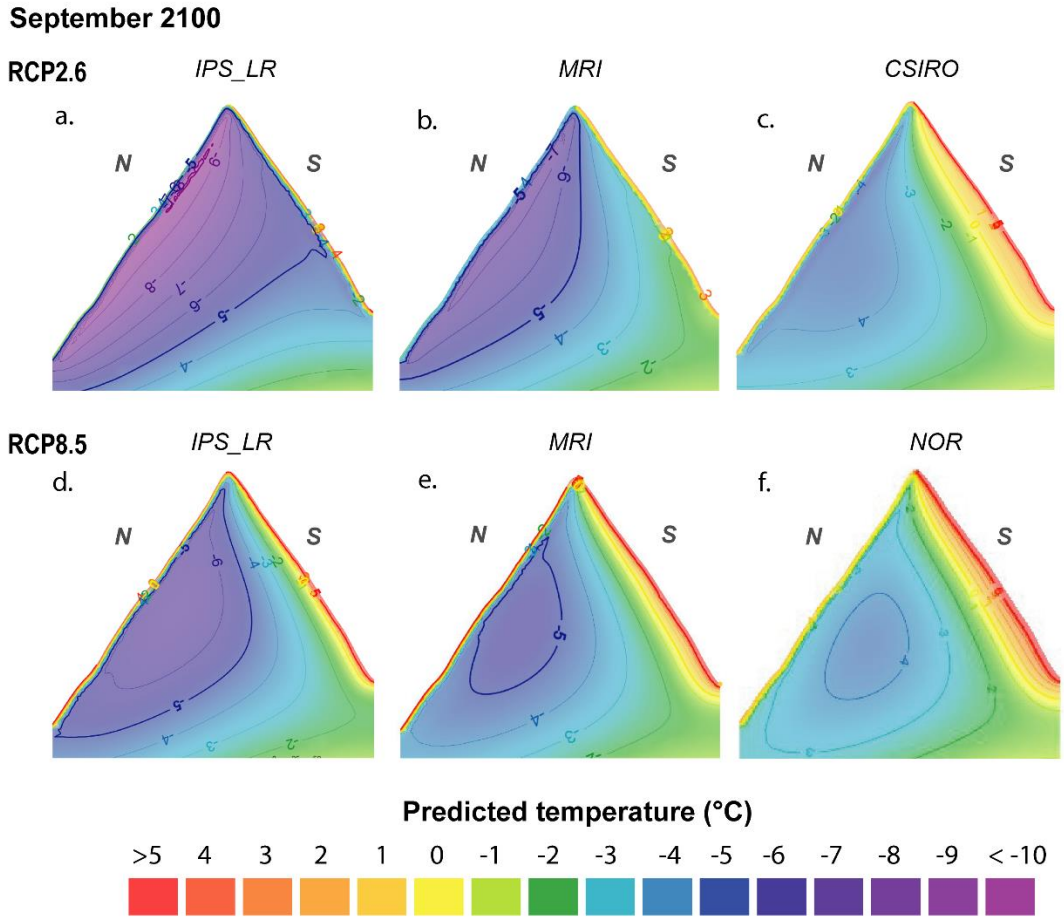

241

242 **Figure 5.** Extreme (95 % confidence interval) and average permafrost predictions in
243 September 2100. High temperature at the very near surfaces (including the NW face) are
244 related to seasonal thawing (i.e. active layer) which is usually near its maximum thickness at
245 this time of the year. IPS_LR (a, d), MRI (b, e), CSIRO (c) and NOR (f) are some of the
246 colder, average and warmer models, respectively, among the 13 used models.

247

248 **Key messages on high elevated permafrost degradation pathways within the 21st century**

249 The Grand Pilier d'Angle is one of the highest and coldest rockwall permafrost site of the
250 European Alps and may be one of the few sites above 4000 m a.s.l. where permafrost will
251 subsist by the end of the 21st century in a "business as usual" scenario. However, under drastic
252 reduction of the greenhouse gas emissions, climate stabilization by the turn of mid-century
253 would significantly slow down the ongoing permafrost degradation.

254 The thermal perturbation caused by atmospheric warming within the first half of the century
255 would be similar whatever the considered RCP (about 1°C), and would affect a depth of about
256 30-40 m below the surface. About 50 and 30% of this perturbation will reach depths of 80 and
257 130 m. However, model uncertainty is as least as high as the predicted average evolution, if not

higher, and firm conclusions are thus limited within this horizon. Current temperature increase is already up to 1°C per decade in alpine bedrock according to Hock et al.[37] and the discrepancy between the projected temperature increase and the observed one within the early 21st century partly results from climate models adjustment compared to air temperature observations. In this respect, predictions are more certain for the second half of the 21st century when model uncertainty is well lower than the projected anomalies and that climate models have aligned with the climate history.

During the second half of the century, bedrock temperature may reach a certain thermal equilibrium under RCP2.6. Such scenario will restrict permafrost thawing where warm permafrost is currently present, *i.e.* below 4000 m a.s.l. for south-facing rock faces, tops of peaks and ridges, and sun-exposed spurs, as well as for north-exposed faces below 3000 m a.s.l.[4,28]. In such scenario, warm permafrost will certainly spread in most of the high-elevation S-facing slopes such as the one of the Grand Pilier d'Angle while cold permafrost conditions will remain in N-facing slopes. However, under a "business as usual scenario", permafrost may almost entirely disappear of most of the alpine rockwalls by 2100 and only subsist in high-elevated (> 4000 m a.s.l.), north-exposed and several tens and even hundreds of meters apart from sun-exposed faces such as the middle of the Grand Pilier d'Angle N face.

These models do not account for a couple of factors contributing to permafrost degradation dampening such as snow deposit in sun-exposed faces[34] or air ventilation in highly fractured bedrock[36]. Such factors may also experience substantial changes in the coming decades and in turn have opposite effects on permafrost dynamics. Snowfall for example, which occur nowadays all year round at high elevation may give way to rainfall in reason of the projected reduction in frost frequency[26]. Instead of protecting the bedrock surface from intense solar radiation[34], this may accelerate permafrost degradation by causing advective heat transport in bedrock clefts[35].

Enhanced permafrost degradation will result in increasing bedrock destabilization with considerable consequences for mountain communities facing endangered practices such as tourism, mountaineering, use of natural resources (e.g. hydroelectricity), and for valley floors due to possible chain reaction hazardous processes[19,22].

Acknowledgments

...

Références

1. French, H. M. Permafrost. in *The Periglacial Environment* 83–115 (John Wiley & Sons, Ltd, 2013). doi:10.1002/9781118684931.ch5.
2. Biskaborn, B. K. *et al.* Permafrost is warming at a global scale. *Nature Communications* **10**, 264 (2019).
3. Williams, P. J. & Smith, M. W. The Frozen Earth: Fundamentals of Geocryology. *Cambridge Core* /core/books/frozen-earth/8232742247427A564DDC0AB2165D10D0 (1989) doi:10.1017/CBO9780511564437.
4. Noetzli, J., Gruber, S., Kohl, T., Salzmann, N. & Haeberli, W. Three-dimensional distribution and evolution of permafrost temperatures in idealized high-mountain topography. *Journal of Geophysical Research: Earth Surface* **112**, (2007).
5. Arenson, L. U., Springman, S. M. & Sego, D. C. The Rheology of Frozen Soils. *Applied Rheology* **17**, 12147–1 (2007).
6. Krautblatter, M., Funk, D. & Günzel, F. K. Why permafrost rocks become unstable: a rock–ice-mechanical model in time and space. *Earth Surface Processes and Landforms* **38**, 876–887 (2013).
7. Bommer, C. & Institut fédéral de recherches sur la forêt, la neige et le paysage (Birmensdorf). *Construire sur le pergélisol: guide pratique*. (Institut fédéral de recherches sur la forêt, la neige et le paysage WSL, 2010).

8. Duvillard, P.-A., Ravanel, L., Marcer, M. & Schoeneich, P. Recent evolution of damage to infrastructure on permafrost in the French Alps. *Reg Environ Change* (2019) doi:10.1007/s10113-019-01465-z.
9. Schiermeier, Q. Alpine thaw breaks ice over permafrost's role | Nature. 712 (2003) doi:https://doi.org/10.1038/424712a.
10. Gruber, S., Hoelzle, M. & Haeberli, W. Permafrost thaw and destabilization of Alpine rock walls in the hot summer of 2003. *Geophysical Research Letters* **31**, (2004).
11. Ravanel, L., Magnin, F. & Deline, P. Impacts of the 2003 and 2015 summer heatwaves on permafrost-affected rock-walls in the Mont Blanc massif. *Science of The Total Environment* **609**, 132–143 (2017).
12. Gruber, S. & Haeberli, W. Permafrost in steep bedrock slopes and its temperature-related destabilization following climate change. *Journal of Geophysical Research: Earth Surface* **112**, (2007).
13. Davies, M. C. R., Hamza, O. & Harris, C. The effect of rise in mean annual temperature on the stability of rock slopes containing ice-filled discontinuities. *Permafrost and Periglacial Processes* **12**, 137–144 (2001).
14. Ravanel, L. & Deline, P. Climate influence on rockfalls in high-Alpine steep rockwalls: The north side of the Aiguilles de Chamonix (Mont Blanc massif) since the end of the 'Little Ice Age'. *The Holocene* **21**, 357–365 (2011).
15. Mourey, J., Marcuzzi, M., Ravanel, L. & Pallandre, F. Effects of climate change on high Alpine mountain environments: Evolution of mountaineering routes in the Mont Blanc massif (Western Alps) over half a century. *Arctic, Antarctic, and Alpine Research* **51**, 176–189 (2019).
16. Ritter, F., Fiebig, M. & Muhar, A. Impacts of Global Warming on Mountaineering: A Classification of Phenomena Affecting the Alpine Trail Network. *mred* **32**, 4–15 (2012).

17. Ravanel, L., Deline, P., Lambiel, C. & Vincent, C. Instability of a High Alpine Rock Ridge: the Lower Arête Des Cosmiques, Mont Blanc Massif, France. *Geografiska Annaler: Series A, Physical Geography* **95**, 51–66 (2013).
18. Huggel, C. *et al.* The 2002 rock/ice avalanche at Kolka/Karmadon, Russian Caucasus: assessment of extraordinary avalanche formation and mobility, and application of QuickBird satellite imagery. *Natural Hazards and Earth System Sciences* **5**, 173–187 (2005).
19. Walter, F. *et al.* Direct observations of a three million cubic meter rock-slope collapse with almost immediate initiation of ensuing debris flows. *Geomorphology* **351**, 106933 (2020).
20. Worni, R., Huggel, C., Clague, J. J., Schaub, Y. & Stoffel, M. Coupling glacial lake impact, dam breach, and flood processes: A modeling perspective. *Geomorphology* **224**, 161–176 (2014).
21. Schaub, Y., Huggel, C. & Cochachin, A. Ice-avalanche scenario elaboration and uncertainty propagation in numerical simulation of rock-/ice-avalanche-induced impact waves at Mount Hualcán and Lake 513, Peru. *Landslides* **13**, 1445–1459 (2016).
22. Haeberli, W., Schaub, Y. & Huggel, C. Increasing risks related to landslides from degrading permafrost into new lakes in de-glaciating mountain ranges. *Geomorphology* **293**, 405–417 (2017).
23. Taylor, K. E., Stouffer, R. J. & Meehl, G. A. An Overview of CMIP5 and the Experiment Design. *Bull. Amer. Meteor. Soc.* **93**, 485–498 (2011).
24. AR5 Climate Change 2013: The Physical Science Basis — IPCC. https://www.ipcc.ch/report/ar5/wg1/.
25. Joly, D. *et al.* Geomatic downscaling of temperatures in the Mont Blanc massif. *International Journal of Climatology* **38**, 1846–1863 (2018).

26. Pohl, B. *et al.* Huge decrease of frost frequency in the Mont-Blanc Massif under climate change. *Sci Rep* **9**, 4919 (2019).
27. Magnin, F., Brenning, A., Bodin, X., Deline, P. & Ravanel, L. Statistical modelling of rock wall permafrost distribution: application to the Mont Blanc massif. *Géomorphologie : relief, processus, environnement* 20 (2015).
28. Magnin, F. *et al.* Modelling rock wall permafrost degradation in the Mont Blanc massif from the LIA to the end of the 21st century. *The Cryosphere* **11**, 1813–1834 (2017).
29. Deline, P., Akçar, N., Ivy-Ochs, S. & Kubik, P. W. Repeated Holocene rock avalanches onto the Brenva Glacier, Mont Blanc massif, Italy: A chronology. *Quaternary Science Reviews* **126**, 186–200 (2015).
30. Deline, P. RECENT BRENVA ROCK AVALANCHES (VALLEY OF AOSTA): NEW CHAPTER IN AN OLD STORY? 9.
31. Noetzli, J. & Gruber, S. Transient thermal effects in Alpine permafrost. *The Cryosphere* **3**, 85–99 (2009).
32. Hipp, T., Etzelmüller, B. & Westermann, S. Permafrost in Alpine Rock Faces from Jotunheimen and Hurrungane, Southern Norway. *Permafrost and Periglacial Processes* **25**, 1–13 (2014).
33. Myhra, K. S., Westermann, S. & Etzelmüller, B. Modelled Distribution and Temporal Evolution of Permafrost in Steep Rock Walls Along a Latitudinal Transect in Norway by CryoGrid 2D. *Permafrost and Periglacial Processes* **28**, 172–182 (2017).
34. Magnin, F. *et al.* Snow control on active layer thickness in steep alpine rock walls (Aiguille du Midi, 3842ma.s.l., Mont Blanc massif). *CATENA* **149**, 648–662 (2017).
35. Hasler, A., Gruber, S., Font, M. & Dubois, A. Advective Heat Transport in Frozen Rock Clefts: Conceptual Model, Laboratory Experiments and Numerical Simulation. *Permafrost and Periglacial Processes* **22**, 378–389 (2011).

36. Hasler, A., Gruber, S. & Haeberli, W. Temperature variability and offset in steep alpine rock and ice faces. *The Cryosphere* **5**, 977–988 (2011).

37. Hock, R. *et al.* Chapter 2: High Mountain Areas — Special Report on the Ocean and Cryosphere in a Changing Climate. https://www.ipcc.ch/srocc/chapter/chapter-2/ (2019).